Recyclable L-Proline Functional Nanoreactors with Temperature-Tuned Activity Based on Core−Shell Nanogels

Annhelen Lu,[†,‖] Dafni Moatsou,[†,‖] Ian Hands-Portman,[‡] Deborah A. Longbottom,[§] and Rachel K. O'Reilly*,[†]

[†]Department of Chemistry, University of Warwick, Gibbet Hill Road, Coventry CV4 7AL, United Kingdom
[‡]School of Life Sciences, University of Warwick, Gibbet Hill Road, Coventry CV4 7AL, United Kingdom
[§]Department of Chemistry, University of Cambridge, Lensfield Road, Cambridge CB2 1EW, United Kingdom

S *Supporting Information*

ABSTRACT: Recyclable core−shell (CS) nanogels based on L-proline-containing hydrophobic cores with a thermoresponsive poly(N-isopropylacrylamide) (PNIPAM) shell have been synthesized via a seeded precipitation polymerization process. Dynamic light scattering (DLS) and transmission electron microscopy (TEM) were used to verify the successful addition of the shell and investigate the thermoresponsive properties of the nanostructures. The catalytic activity of the nanogels was assessed in a model asymmetric aldol reaction, where an enhancement was observed with increasing temperature, attributed to the hydrophobic nature of the PNIPAM shell. However, when a nanogel was synthesized with core−shell morphology based on a gradient of cross-linking density in the corona (GS), a dramatic drop in activity was observed at elevated temperatures: the collapse of the outer, lightly cross-linked, "corona" polymer chains appears to block access to the catalytic core. High activity and enantioselectivity were maintained in a number of recovery and reuse cycles, highlighting the recycling potential of these catalytic nanostructures.
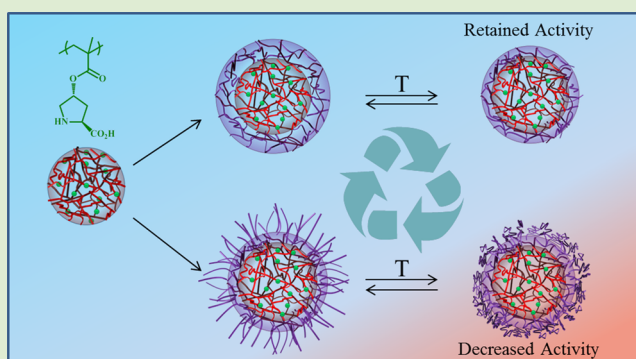
In Nature, aldolase enzymes carry out highly enantioselective carbon−carbon bond forming reactions in a controlled fashion within small hydrophobic pockets.[1] Numerous synthetic systems have been designed to mimic the natural ones,[1−7] from single-molecule catalytic species[8−10] to compartment-forming ones,[11] in which catalytic functionalities such as transition metals or organocatalysts have been introduced to yield highly efficient nanoreactors.[10,12−27] An enhancement in catalytic activity is often observed in these systems as a result of the efficient concentration of organic substrates within the hydrophobic cavity, an effect known as the concentrator effect.[28] The hydrophobic cavity within nanostructures has also been used to accommodate a range of lipophilic molecules such as dyes and drugs, in water.[29−32] A very popular organocatalyst incorporated into such systems is the amino acid L-proline,[23,33−39] and our group has previously shown its successful incorporation into the hydrophobic core of a range of novel polymeric nanostructures.[40−43] High catalyst activity was reported for the aldol reaction between two relatively hydrophobic substrates, in water, which does not occur at all with the native catalyst in the same medium.[44]

Catalyst loading has been significantly lowered in many of the systems, and significant advances have now been made in terms of carrying out reactions in aqueous media; however, there is still room for improvement and extension to what is possible in the area of designing structurally well-defined and readily recyclable nanoreactor systems.[45] Poly(N-isopropylacrylamide) (PNIPAM) is a well-studied thermoresponsive polymer with a lower critical solution temperature (LCST) of approximately 32 °C,[46,47] a property which has been utilized in a number of recyclable catalytic systems, where recovery has been achieved by precipitation at elevated temperatures.[48,49] The change in solubility of the polymer in water around its LCST has been explored to allow for switching between unimer and micellar states which in turn modulate the catalytic activity.[40] Cross-linked PNIPAM microgels have also been used as intelligent microreactors where the reversible hydrophobic nature of PNIPAM as a response to temperature has been used to control access of substrates into the catalytic core. In some cases, enhanced catalytic activity is observed at elevated temperatures as the hydrophobic nature of PNIPAM enhances substrate uptake.[50,51] In other cases, the opposite effect has been reported where the collapse of PNIPAM instead blocks the catalytic sites and thus reduces nanoreactor activity.[52,53] Several groups have successfully taken advantage of both the hydrophilic and hydrophobic properties of PNIPAM, allowing

catalysis of both hydrophilic and hydrophobic substrates by simply tuning the temperature of the system.[25,54]

We wanted to expand on this by synthesizing L-proline-containing thermoresponsive nanogels, the catalyst being contained in a hydrophobic core while the shell is temperature responsive, and investigate the catalytic activity and selectivity dependency on temperature. Thus, two PNIPAM shells with different morphologies were synthesized to investigate the effect of their collapse on the activity of the core-functionalized catalyst. The first system consisted of the catalytic core surrounded by a cross-linked PNIPAM shell (CS) and the second by a thinner cross-linked shell and a "corona" made up of less cross-linked PNIPAM polymer chains, essentially resulting in a decreasing gradient of cross-linking density (GS). We hypothesized that the less cross-linked PNIPAM chains would collapse in a different manner to the cross-linked PNIPAM network at elevated temperatures and that this might yield two nanoreactor systems with unique and tunable catalytic efficiencies.

First, based on findings from our previous studies,[41] the hydrophobic core, containing the catalytic L-proline functionality (seed), was synthesized by emulsion copolymerization of ethyl methacrylate (EMA), proline methacrylate (ProMA), and ethylene glycol dimethacrylate (EGDMA), resulting in particles with an average 35 nm diameter, incorporating (based on the monomer feed ratios) 15 wt % of catalyst functionalization (DoF) and 0.5 wt % cross-linking density (CLD) (DLS, TEM in Supporting Information (SI), Figures S2 and S3). The thermoresponsive core-cross-linked shell (CS) nanogels were then synthesized, using our catalytic seeds and following a well-established seeded precipitation polymerization procedure.[55−60] Similarly, the core−gradient shell (GS) morphology was pursued by initially allowing the polymerization of a cross-linked shell using half the volume of reagents compared to that used for the CS particles, followed by the addition of the remaining monomer without additional cross-linker or initiator (Figures S1 and S8, SI). We hypothesize that the polymerization of the second batch of monomer proceeds from the remaining radicals in solution, although further investigation into the mechanism is ongoing.

In the CS case, the increase in size of the nanogels from 35 to 132 nm upon addition of NIPAM/cross-linker is prominent and attributed to formation of the desired cross-linked PNIPAM shell (Figure 1A). Similarly, for the GS nanogels, upon addition of the first batch of NIPAM monomer (with cross-linker), an increase in particle hydrodynamic diameter (D_h) was seen by DLS (Figure 1B), followed by a further increase in D_h upon addition of the second batch of NIPAM (no cross-linking agent), suggesting a two-step shell addition. Due to the thermoresponsive nature of PNIPAM, particle growth was monitored by removing samples and performing the measurements at 5 °C, in order to easily observe the change in D_h (SI, Figure S8 and Table S1) at a temperature where the PNIPAM shell is fully hydrated. At the end of the polymerization, an overall change in D_h from 35 nm to 132 and 142 nm was observed for CS and GS nanogels, respectively (Figure 1). The lack of a small population (by DLS) suggests complete functionalization of the seed particles as well as the absence of NIPAM homopolymer, though further investigation is necessary to prove this beyond doubt.

In order to further investigate the CS and GS morphology the particles were observed by TEM. Unsurprisingly, dry-state TEM was not conclusive, as water is effectively removed from
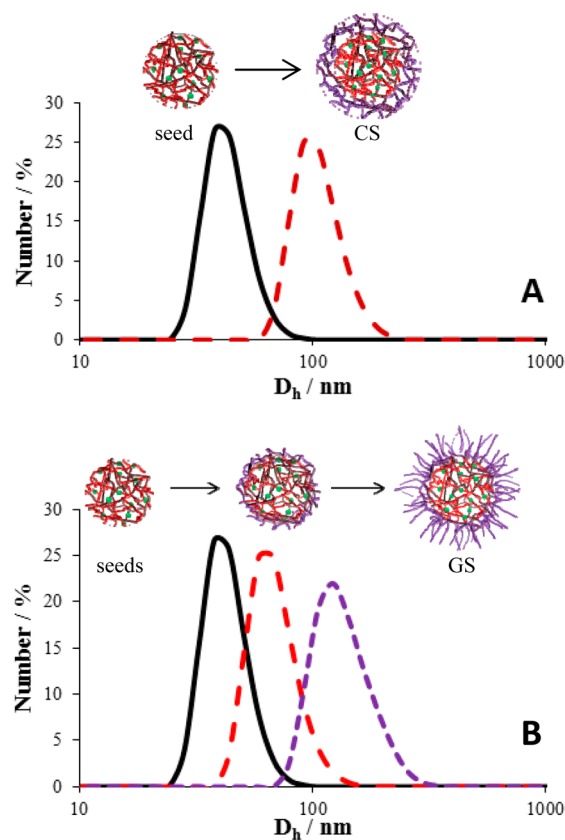

Figure 1. DLS traces of hydrophobic EMA core (black trace) and the corresponding thinner CS (A, red trace) and GS (B, purple trace) nanogels upon addition of a PNIPAM shell/corona, determined at 5 °C.

the shell upon deposition onto the TEM grid causing it to collapse onto the core; thus, spherical particles with an average size of 39 and 38 nm, respectively, were observed (SI, Figures S5 and S9), which is a minor increase in particle size compared to the seed particles. Nevertheless, when observed with cryogenic TEM (SI, Figures S7 and S11) and selective staining of PNIPAM (SI, Figures S6 and S10), the CS and GS particles both appeared to have a core−shell morphology, suggesting the successful seeded polymerization of NIPAM.

As previously mentioned, PNIPAM exhibits an LCST at about 32 °C, below which it is hydrophilic and water-soluble and above which it becomes hydrophobic and collapses. The change in particle size with respect to temperature was investigated by DLS. As expected, for both morphologies a decrease in D_h was observed with increasing temperature as water is removed from the shell causing PNIPAM to collapse and thus the shell to shrink (Figure 2 and SI Figure S17). A further nanogel CS-50, with 50 wt % shell cross-linking (DLS, TEM in SI Figures S12 and S13), was also investigated (Figure 2), and as expected it demonstrated a smaller change in size upon heating compared to CS and GS. The transition temperature, where the most significant change in size is observed, was more accurately determined using the first derivative[59] of the change in D_h with temperature and was found to be 30, 27, and 33 °C for CS, GS, and CS-50, respectively (SI, Figures S18 and S19). The reversible change in particle D_h which results from the temperature-dependent hydrophobic and hydrophilic nature of the shell was confirmed by exposing the nanostructures to repeated heating and cooling
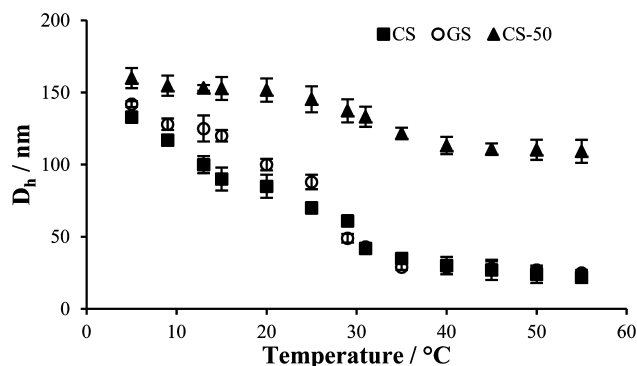
Figure 2. Change in D_h with temperature, confirming the shrinking of the PNIPAM shell with increasing temperature (error bars are from standard deviation).
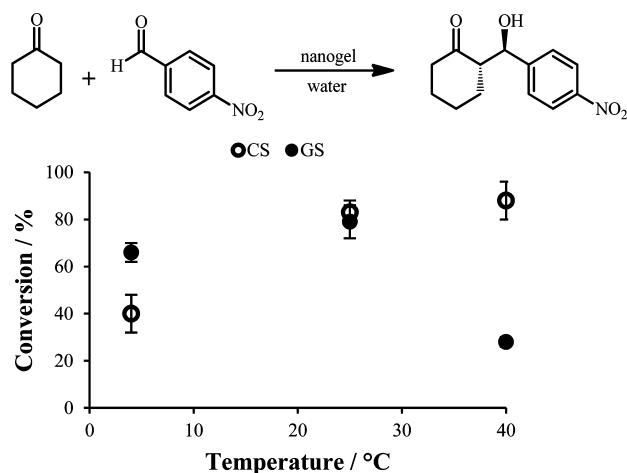

Figure 3. Conversion of asymmetric aldol reaction catalyzed by CS and GS at 2 mol % loading and three different temperatures, determined after 24 h (all experiments were performed in triplicate).

cycles, achieving comparable particle sizes in multiple cycles (SI, Figure S20).

Because the TEM data did not differentiate between the two targeted morphologies, it was proposed that in the case of the GS nanogels the second batch of NIPAM may simply have diffused into the cross-linked shell and polymerized within it, rather than forming an extra layer of PNIPAM chains. To assess the possibility of that happening, we examined the polymerization of NIPAM in the presence of a preformed CS nanogel. These nanogels (ICS) were found to indeed increase in size (SI, Figures S14−S16), attributed to the polymerization of NIPAM within the PNIPAM shell. This kind of morphology is expected to render the shell more rigid and therefore shrink less upon heating. Indeed, upon heating the ICS particles decreased in size, shrinking to 50% of their original size, whereas the GS shell reached 19% of their swollen size (SI, Figure S21). In addition to that, at elevated temperatures the CS-50 nanogel is significantly larger, shrinking to only 68% of its original size, a value much larger than either that of the CS (which was 17%) or GS but more comparable to that of the PNIPAM-impregnated ICS nanogels. This further suggests that the GS nanogels do not demonstrate the same rigidity as the purposely heavily cross-linked CS-50 nanogels nor that of the ICS particles, thus supporting the suggested gradient cross-linked shell morphology.

The efficiency of the core−shell nanostructures as nano-reactors in water was investigated in a model asymmetric aldol reaction[38,42,61] between 4-nitrobenzaldehyde and cyclohexanone (Figure 3). We hypothesized that the collapse of cross-linked PNIPAM in the CS and GS case would differ, potentially resulting in different catalytic efficiencies at elevated temperatures. In order to examine the catalytic dependency of the nanostructures on temperature, reactions were carried out at three temperatures: at 4 °C where PNIPAM is in a hydrophilic and fully solvated state, at around room temperature, 25 °C where PNIPAM is somewhat hydrophobic, and finally at 40 °C where it is fully hydrophobic and in a collapsed state. Catalysis was carried out as previously reported[41] at 2 mol % catalyst loading, and a differing temperature-dependent catalytic activity was indeed observed for both nanogel systems. At low temperature, GS showed appreciably greater catalytic activity than the corresponding CS nanogel (66 vs 40% conversion), which was attributed to the lower cross-linking density of the GS shell, effectively resembling more the morphology of micelles whose catalytic activity is found to be high.[21,40,43] At 25 °C, the conversion increases and is comparable for both

systems; however, at elevated temperature they display the converse behavior, with CS displaying greater activity than their GS counterparts (88 vs 28% conversion, Figure 3). The CS nanogels followed an Arrhenius-type dependence on temperature,[62] where an increase in catalytic activity was observed with increasing temperature, which may be due to an increase in substrate uptake as a result of the increased hydrophobicity of PNIPAM at high temperature and the greater mobility of the substrates within the core. While this is not in agreement with the literature,[63] we believe it is a demonstration of the absence of water within the hydrophobic core. GS on the other hand showed a significant drop in activity at elevated temperatures with a decrease in conversion from 79% at 25 °C to 28% at 40 °C (Table 1). This is consistent with the hypothesis that the

Table 1. Catalytic Efficiency of CS and GS at 2 mol % Loading and Three Different Temperatures

catalyst	T/°C	$D_h{}^a$/nm	conv.[b]/%		anti/syn ratio[b]		ee[c]/%	
CS	4	133	40	±8	98/2	±1	86	±2
	25	70	83	±5	97/3	±1	93	±2
	40	30	88	±8	96/4	±1	96	±1
GS	4	142	66	±4	96/4	±2	95	±1
	25	88	79	±7	97/3	±1	95	±1
	40	28	28	±2	95/5	±3	97	±1

[a]Determined by DLS. [b]Determined by ^{1}H NMR spectroscopy after 24 h (400 MHz, CDCl$_3$), reactions carried out in triplicate. [c]Determined by HPLC, ChiralPak IA, hexane:propan-2-ol:ethanol (80:10:10).

less cross-linked polymer chains of the GS shell collapse in a different manner to the consistently cross-linked CS shell and seem to block access to the core rather than enhance substrate uptake. Except for a slightly lower enantioselectivity (ee) for CS nanogels at 4 °C, both nanogel systems are highly enantioselective, highlighting the successful design of our nanostructure for efficient enantioselective organocatalysis in water (Table 1).

For comparison, a drop in conversion was not observed at 40 °C when CS-50 was used (SI Table S2), suggesting a simple increase in shell density cannot be used to explain the properties observed by GS. Thus, we maintain our hypothesis that the shell morphology of the CS and GS nanogels differs, whereby the CS is constructed by a hydrophobic cross-linked

core and a temperature-responsive cross-linked shell, while the GS morphology bears an additional layer where the polymer chains are more flexible. This morphological difference is then directly linked to their catalytic activity.

One of the main motivations behind the design and synthesis of these CS and GS nanoreactors is their potential recyclability, an important feature to take into account due to the high catalyst loadings (~30 mol %) often required in conventional organocatalytic reactions.[61,64] For this purpose, the solubility of PNIPAM in water at temperatures below its LCST was used. Organic reagents/products were removed from the nanogel core via extraction with diethyl ether, after which the remaining aqueous solution containing the nanogels was dried and subsequently redispersed into water at 4 °C. In terms of particle size, a similar D_h was observed for both the CS and GS nanogels before and after catalysis (SI, Figure S22), though some larger structures were observed after the sixth catalytic cycle (SI, Figure S23). In terms of catalytic activity, the recovery and redispersion process provided high catalytic efficiencies, with conversion only deteriorating after the fourth cycle (Figure 4 and SI, Table S3). This may be attributed to
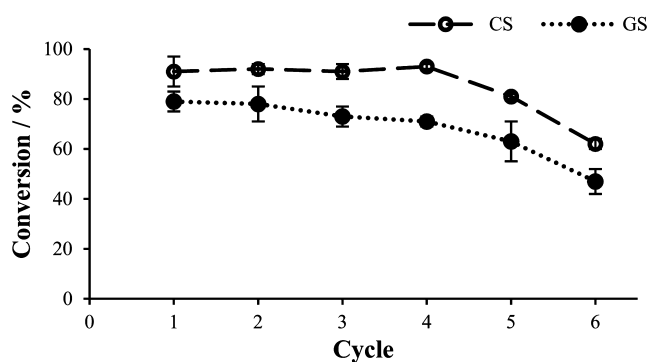

Figure 4. Catalytic efficiency of the CS and GC nanogels over six cycles, carried out at 2 mol % loading and 25 °C, determined by ^{1}H NMR spectroscopy after 24 h (all experiments were performed in triplicate).

small losses of nanogels after each catalytic cycle and was not seen to be problematic overall, as the reaction goes to completion if allowed to run for an additional 12–24 h. In addition, enantioselectivity was maintained by both nanogels throughout with only a small drop from 97% to 87% and 95% to 87% ee for CS and GS, respectively, after six catalytic cycles (SI, Table S3). This suggests the nanogels act as excellent scaffolds for L-proline-catalyzed reactions in water.

To conclude, in this work we have successfully synthesized recyclable core–shell and core–shell-corona type nanostructures in a simple two-step procedure, through emulsion polymerization of the hydrophobic core followed by a seeded precipitation polymerization to form the shell. The morphology of the thermoresponsive PNIPAM shell was found to have a significant effect on the activity of the catalyst embedded within the hydrophobic core: indeed collapse of PNIPAM at elevated temperatures was found to increase the catalytic activity of nanogels with a CS morphology (attributed to the increased hydrophobic nature of the CS nanogels), whereas collapse of the less cross-linked PNIPAM corona in the GS nanogels appears to block substrate access to the catalytic core resulting in a dramatic drop in activity. Interestingly, high enantioselectivity was maintained in both systems throughout, as well as

in a number of recovery and reuse cycles, highlighting the recycling potential of these novel catalytic nanostructures.

■ ASSOCIATED CONTENT

Ⓢ Supporting Information

Synthetic procedures and some characterizations are also provided. This material is available free of charge via the Internet at http://pubs.acs.org.

■ AUTHOR INFORMATION

Corresponding Author
*E-mail: r.k.o-reilly@warwick.ac.uk.

Author Contributions
‖These authors contributed equally.

Notes
The authors declare no competing financial interest.

■ ACKNOWLEDGMENTS

■ REFERENCES

(1) Machajewski, T. D.; Wong, C.-H. *Angew. Chem., Int. Ed.* **2000**, *39*, 1352−1375.
(2) Mlynarski, J.; Bas, S. *Chem. Soc. Rev.* **2014**, *43*, 577−587.
(3) Bhowmick, S.; Bhowmick, K. C. *Tetrahedron: Asymmetry* **2011**, *22*, 1945−1979.
(4) Gröger, H.; Hummel, W. *Curr. Opin. Chem. Biol.* **2014**, *19*, 171−179.
(5) Mase, N.; Barbas, C. F., III *Org. Biomol. Chem.* **2010**, *8*, 4043−4050.
(6) Raj, M.; Singh, V. K. *Chem. Commun. (Cambridge, U. K.)* **2009**, 6687−6703.
(7) Zhao, Q.; Lam, Y.-h.; Kheirabadi, M.; Xu, C.; Houk, K. N.; Schafmeister, C. E. *J. Org. Chem.* **2012**, *77*, 4784−4792.
(8) Artar, M.; Terashima, T.; Sawamoto, M.; Meijer, E. W.; Palmans, A. R. A. *J. Polym. Sci., Part A: Polym. Chem.* **2014**, *52*, 12−20.
(9) Helms, B.; Fréchet, J. M. J. *Adv. Synth. Catal.* **2006**, *348*, 1125−1148.
(10) Helms, B.; Guillaudeu, S. J.; Xie, Y.; McMurdo, M.; Hawker, C. J.; Fréchet, J. M. J. *Angew. Chem., Int. Ed.* **2005**, *44*, 6384−6387.
(11) Peters, R. J. R. W.; Louzao, I.; van Hest, J. C. M. *Chem. Sci.* **2012**, *3*, 335−342.
(12) Moore, B. L.; Moatsou, D.; Lu, A.; O'Reilly, R. K. *Polym. Chem.* **2014**, *5*, 3487−3494.
(13) Terashima, T.; Nomura, A.; Ito, M.; Ouchi, M.; Sawamoto, M. *Angew. Chem., Int. Ed.* **2011**, *50*, 7892−7895.
(14) Terashima, T.; Nomura, A.; Ouchi, M.; Sawamoto, M. *Macromol. Rapid Commun.* **2012**, *33*, 833−841.
(15) Liu, Y.; Wang, Y.; Wang, Y.; Lu, J.; Piñón, V.; Weck, M. *J. Am. Chem. Soc.* **2011**, *133*, 14260−14263.
(16) Cotanda, P.; Lu, A.; Patterson, J. P.; Petzetakis, N.; O'Reilly, R. K. *Macromolecules* **2012**, *45*, 2377−2384.
(17) Berdugo, C.; Miravet, J. F.; Escuder, B. *Chem. Commun.* **2013**, *49*, 10608−10610.
(18) Lu, A.; O'Reilly, R. K. *Curr. Opin. Biotechnol.* **2013**, *24*, 639−645.
(19) Patterson, J. P.; Cotanda, P.; Kelley, E. G.; Moughton, A. O.; Lu, A.; Epps, T. H., III; O'Reilly, R. K. *Polym. Chem.* **2013**, *4*, 2033−2039.
(20) Ievins, A. D.; Wang, X.; Moughton, A. O.; Skey, J.; O'Reilly, R. K. *Macromolecules* **2008**, *41*, 2998−3006.

(21) Huerta, E.; Stals, P. J. M.; Meijer, E. W.; Palmans, A. R. A. *Angew. Chem., Int. Ed.* **2013**, *52*, 2906−2910.

(22) Wu, Y.; Zhang, Y.; Yu, M.; Zhao, G.; Wang, S. *Org. Lett.* **2006**, *8*, 4417−4420.

(23) Lipshutz, B. H.; Ghorai, S. *Org. Lett.* **2011**, *14*, 422−425.

(24) Doyagüez, E. G.; Rodríguez-Hernández, J.; Corrales, G.; Fernández-Mayoralas, A.; Gallardo, A. *Macromolecules* **2012**, *45*, 7676−7683.

(25) Valade, D.; Jeon, Y.; Kessel, S.; Monteiro, M. J. *J. Polym. Sci. A, Polym. Chem.* **2012**, *50*, 4762−4771.

(26) Diallo, A. K.; Boisselier, E.; Liang, L.; Ruiz, J.; Astruc, D. *Chem.−Eur. J.* **2010**, *16*, 11832−11835.

(27) Lan, Y.; Yang, L.; Zhang, M.; Zhang, W.; Wang, S. *ACS Appl. Mater. Interfaces* **2009**, *2*, 127−133.

(28) Helms, B.; Liang, C. O.; Hawker, C. J.; Fréchet, J. M. J. *Macromolecules* **2005**, *38*, 5411−5415.

(29) Ryu, J.-H.; Jiwpanich, S.; Chacko, R.; Bickerton, S.; Thayumanavan, S. *J. Am. Chem. Soc.* **2010**, *132*, 8246−8247.

(30) González-Toro, D. C.; Ryu, J.-H.; Chacko, R. T.; Zhuang, J.; Thayumanavan, S. *J. Am. Chem. Soc.* **2012**, *134*, 6964−6967.

(31) Koda, Y.; Terashima, T.; Nomura, A.; Ouchi, M.; Sawamoto, M. *Macromolecules* **2011**, *44*, 4574−4578.

(32) Xu, J.; Chen, G.; Yan, R.; Wang, D.; Zhang, M.; Zhang, W.; Sun, P. *Macromolecules* **2011**, *44*, 3730−3738.

(33) List, B. *Tetrahedron* **2002**, *58*, 5573−5590.

(34) Hayashi, Y.; Sumiya, T.; Takahashi, J.; Gotoh, H.; Urushima, T.; Shoji, M. *Angew. Chem., Int. Ed.* **2006**, *45*, 958−961.

(35) Aratake, S.; Itoh, T.; Okano, T.; Nagae, N.; Sumiya, T.; Shoji, M.; Hayashi, Y. *Chem.−Eur. J.* **2007**, *13*, 10246−10256.

(36) Kristensen, T. E.; Hansen, F. K.; Hansen, T. *Eur. J. Org. Chem.* **2009**, 387−395.

(37) Kristensen, T. E.; Vestli, K.; Fredriksen, K. A.; Hansen, F. K.; Hansen, T. *Org. Lett.* **2009**, *11*, 2968−2971.

(38) Gruttadauria, M.; Giacalone, F.; Mossuto Marculescu, A.; Lo Meo, P.; Riela, S.; Noto, R. *Eur. J. Org. Chem.* **2007**, 4688−4698.

(39) Mase, N.; Nakai, Y.; Ohara, N.; Yoda, H.; Takabe, K.; Tanaka, F.; Barbas, C. F., III *J. Am. Chem. Soc.* **2005**, *128*, 734−735.

(40) Zayas, H. A.; Lu, A.; Valade, D.; Amir, F.; Jia, Z.; O'Reilly, R. K.; Monteiro, M. J. *ACS Macro Lett.* **2013**, *2*, 327−331.

(41) Lu, A.; Moatsou, D.; Longbottom, D. A.; O'Reilly, R. K. *Chem. Sci.* **2013**, *4*, 965−969.

(42) Lu, A.; Smart, T. P.; Epps, T. H., III; Longbottom, D. A.; O'Reilly, R. K. *Macromolecules* **2011**, *44*, 7233−7241.

(43) Lu, A.; Cotanda, P.; Patterson, J. P.; Longbottom, D. A.; O'Reilly, R. K. *Chem. Commun.* **2012**, *48*, 9699−9701.

(44) Hayashi, Y.; Sumiya, T.; Takahashi, J.; Gotoh, H.; Urushima, T.; Shoji, M. *Angew. Chem.* **2006**, *118*, 972−975.

(45) Zhang, J.; Zhang, M.; Tang, K.; Verpoort, F.; Sun, T. *Small* **2014**, *10*, 32−46.

(46) Schild, H. G. *Prog. Polym. Sci.* **1992**, *17*, 163−249.

(47) Heskins, M.; Guillet, J. E. *J. Macromol. Sci. A* **1968**, *2*, 1441−1455.

(48) Bergbreiter, D. E. *Catal. Today* **1998**, *42*, 389−397.

(49) Bergbreiter, D. E.; Osburn, P. L.; Li, C. *Org. Lett.* **2002**, *4*, 737−740.

(50) Ge, Z.; Xie, D.; Chen, D.; Jiang, X.; Zhang, Y.; Liu, H.; Liu, S. *Macromolecules* **2007**, *40*, 3538−3546.

(51) Lu, Y.; Proch, S.; Schrinner, M.; Drechsler, M.; Kempe, R.; Ballauff, M. *J. Mater. Chem.* **2009**, *19*, 3955−3961.

(52) Carregal-Romero, S.; Buurma, N. J.; Pérez-Juste, J.; Liz-Marzán, L. M.; Hervés, P. *Chem. Mater.* **2010**, *22*, 3051−3059.

(53) Lu, Y.; Yuan, J.; Polzer, F.; Drechsler, M.; Preussner, J. *ACS Nano* **2010**, *4*, 7078−7086.

(54) Wei, G.; Zhang, W.; Wen, F.; Wang, Y.; Zhang, M. *J. Phys. Chem. C* **2008**, *112*, 10827−10832.

(55) Makino, K.; Yamamoto, S.; Fujimoto, K.; Kawaguchi, H.; Ohshima, H. *J. Colloid Interface Sci.* **1994**, *166*, 251−258.

(56) Saunders, B. R.; Crowther, H. M.; Vincent, B. *Macromolecules* **1997**, *30*, 482−487.

(57) Berndt, I.; Richtering, W. *Macromolecules* **2003**, *36*, 8780−8785.

(58) Jones, C. D.; Lyon, L. A. *Macromolecules* **2000**, *33*, 8301−8306.

(59) Balaceanu, A.; Verkh, Y.; Demco, D. E.; Möller, M.; Pich, A. *Macromolecules* **2013**, *46*, 4882−4891.

(60) Hellweg, T.; Dewhurst, C. D.; Eimer, W.; Kratz, K. *Langmuir* **2004**, *20*, 4330−4335.

(61) Sakthivel, K.; Notz, W.; Bui, T.; Barbas, C. F., III *J. Am. Chem. Soc.* **2001**, *123*, 5260−5267.

(62) Li, S.; Ge, Y.; Tiwari, A.; Cao, S. *Small* **2010**, *6*, 2453−2459.

(63) Emer, E.; Galletti, P.; Giacomini, D. *Tetrahedron* **2008**, *64*, 11205−11208.

(64) List, B.; Lerner, R. A.; Barbas, C. F., III *J. Am. Chem. Soc.* **2000**, *122*, 2395−2396.